NUCL SCI TECH (2020) 31:123
https://doi.org/10.1007/s41365-020-00832-4

Secondary decay effects of the isospin fractionation in the projectile fragmentation at GeV/nucleon

Chen-Chen Guo[1] · Jun Su[1] · Long Zhu[1]

Received: 29 May 2020 / Revised: 28 October 2020 / Accepted: 3 November 2020 / Published online: 5 December 2020

Abstract The isospin fractionations in ^{124}Sn, ^{107}Sn + ^{120}Sn at 600 MeV/nucleon, and ^{136}Xe, ^{124}Xe + ^{208}Pb at 1000 MeV/nucleon are investigated by the isospin-dependent quantum molecular dynamics model coupled with the statistical code GEMINI. The yield ratio as a function of the binding energy difference for light mirror nuclei ^{3}H/^{3}He, ^{7}Li/^{7}Be, ^{11}B/^{11}C, and ^{15}N/^{15}O is applied to estimate the ratio between neutrons and protons in the gas of the fragmenting system. By comparing the estimated values resulting from the simulations with and without the GEMINI code, it was found that the secondary decay distorts the signal of the isospin fractionation. To minimize the secondary decay effects, the yield ratio of the light mirror nuclei ^{3}H/^{3}He as well as its double ratio between two systems with different isospin asymmetries of the projectiles is recommended as robust isospin observables.

Keywords Quantum molecular dynamics model (QMD) · Isospin fractionation · Secondary decay effect

This work was supported by the Natural Science Foundation of China under (Nos. U2032137 and U1832182), the Natural Science Foundation of Guangdong Province, China (No.18zxxt65), and Fundamental Research Funds for the Central Universities (No. 19lgpy306).

✉ Chen-Chen Guo
guochch7@mail.sysu.edu.cn

1 Sino-French Institute of Nuclear Engineering and Technology, Sun Yat-sen University, Zhuhai 519082, China

1 Introduction

Investigations on fractionation have stimulated significant theoretical and experimental efforts in many branches of science and technology [1, 2]. In recent years, there has been increasing interest in nuclear isospin fractionation, which indicates the separation of neutron-rich gas during a liquid-gas phase transition in nuclear matter [3–6]. It was reported in the early 1980s although the concept of isospin fractionation was not applied. For example, it was found that fragment emission amplified the ratio of free neutrons to protons relative to that in the total system [7]. In 2000, the concept of isospin fractionation was used to describe the measurement of the isotopic distributions of light particles and intermediate mass fragments in the collisions between tin isotopes at 50 MeV/nucleon [8]. Isospin fractionation is an important phenomenon in heavy ion collisions in the energy region from the Fermi energy to giga-electron volt. It has been proposed that the observable associated with the isospin fractionation is sensitive to the isospin dependence of the nuclear equation-of-state in isospin-asymmetric nuclear matter [9–11]. The differential isospin fractionation is also considered to be significantly affected by the isospin splitting of the nucleon effective mass [12, 13].

Several dynamical effects on the isospin fractionation have been studied. For example, the effect of Coulomb interaction on the isospin fractionation has received attention [14–16]. The relationship between fragment chemical composition and the expected isospin fractionation has also been explored [17]. However, studies on the secondary decay effects remain few. Isospin fractionation occurs during the fragmenting process in heavy ion collisions that form excited fragments [18–22]. The decay of these excited fragments changes the isospin asymmetry of the gas (free nucleons) and liquid (fragments) phases [23, 24]. Thus, the secondary decay effects should be considered when comparing model calculations with experimental data. In our previous work, the dynamic properties, secondary decay effects, and isospin dependence of projectile fragmentations in ^{124}Sn, ^{107}Sn + ^{120}Sn collisions at 600 MeV/nucleon were studied by an isospin-dependent quantum molecular dynamics (IQMD) model coupled with the statistical code GEMINI [25–27]. In this work, the isospin fractionation and its secondary decay effects are studied using a momentum-dependent potential version of the IQMD model [28, 29] coupled with the GEMINI code. The method is introduced briefly in Sect. 2. The results and discussions are presented in Sect. 3. Finally, a summary is given in Sect. 4.

2 Theoretical method

The theoretical description is provided in detail in Ref. [25]. Here, the main parts of the model are emphasized. The version of the IQMD model is the IQMD-BNU (Beijing Normal University).

The nuclear interaction is described by the potential energy density of asymmetric nuclear matter with density ρ and asymmetry δ:

$$\begin{aligned} V(\rho,\delta) = {} & \frac{\alpha}{2}\frac{\rho^2}{\rho_0} + \frac{\beta}{\gamma+1}\frac{\rho^{\gamma+1}}{\rho_0^{\gamma}} + \frac{C_{sp}}{2}\left(\frac{\rho}{\rho_0}\right)^{\gamma_i}\rho\delta^2, \\ & + \sum_{\tau}(1+x)\iint v(\mathbf{p},\mathbf{p}')f_{\tau}(\mathbf{r},\mathbf{p})f_{\tau}(\mathbf{r},\mathbf{p}')\mathrm{d}\mathbf{p}\mathrm{d}\mathbf{p}' \\ & + \sum_{\tau}(1-x)\iint v(\mathbf{p},\mathbf{p}')f_{\tau}(\mathbf{r},\mathbf{p})f_{-\tau}(\mathbf{r},\mathbf{p}')\mathrm{d}\mathbf{p}\mathrm{d}\mathbf{p}', \\ v(\mathbf{p},\mathbf{p}') = {} & \frac{C_m/\rho_0}{1+(\mathbf{p}-\mathbf{p}')^2/\Lambda^2}, \end{aligned} \tag{1}$$

where $\rho_0 = 0.16$ fm^{-3} is the normal density; $\mathbf{p}$ and $\mathbf{p}'$ are the momenta of the nucleon; and $f_{\tau}(\mathbf{r},\mathbf{p})$ is the phase-space density, with $\tau = 1/2$ for the neutrons and $\tau = -1/2$ for the protons. The parameters $\alpha = -75.86$ MeV, $\beta = 166.43$ MeV, $\gamma = 1.226$, $C_{sp} = 38.06$ MeV, $x = 0$, $C_m = -88.21$ MeV, and $\Lambda = 664.86$ MeV/c are temperature-independent, while the phase-space density is temperature-dependent. The parameter $\gamma_i = 0.35$, 0.75, and 2 will be applied to the corresponding slope of the symmetry energy at normal density of 45.12, 67.96, and 139.32 MeV, respectively.

Binary nucleon–nucleon (NN) collisions depend on the differential cross section of NN collisions. The cross section of NN collisions in free space was taken from Ref. [30]. The in-medium correction of the cross section is considered by [31]

$$\begin{aligned} f_{\mathrm{el}}^{\mathrm{med}} &= \sigma_0/\sigma^{\mathrm{free}}\tanh(\sigma^{\mathrm{free}}/\sigma_0), \\ \sigma_0 &= 0.85\rho^{-2/3}. \end{aligned} \tag{2}$$

The phase-space density constraint (PSDC) method is applied to compensate for the fermionic feature. The phase-space occupation probability $\bar{f}_i$ is calculated at each time step. The PSDC approach is the same as that of CoMD [32, 33].

$$\begin{aligned} \bar{f}_i = {} & \int_{h^3}\frac{1}{\pi^3\hbar^3}\mathrm{d}^3r\mathrm{d}^3p \\ & + \frac{1}{2}\sum_{j=1,j\neq i}^{N}\delta_{\tau_j,\tau_i}\int_{h^3}\frac{1}{\pi^3\hbar^3}e^{-\frac{(\mathbf{r}_j-\mathbf{r}_i)^2}{2L}-\frac{(\mathbf{p}_j-\mathbf{p}_i)^2 2L}{\hbar^2}}\mathrm{d}^3r\mathrm{d}^3p, \end{aligned} \tag{3}$$

where δ_{τ_j,τ_i} is the delta function. When $\tau_j = \tau_i$, the function is equal to 1; otherwise, it is 0. τ_i represents the isospin degree-of-freedom. In the mean-field evolution, the momentum of each nucleon is randomly changed by many-body elastic scattering if its phase-space occupation $\bar{f}_i$ is greater than 1. In binary NN collisions, only the scattering that results in the final state with a phase-space occupation of less than 1 is allowed.

The evolution by the IQMD model is stopped, and the GEMINI code is switched on when the excitation energy of the prefragments is less than a specified value $E_{\mathrm{stop}} = 3$ MeV/nucleon. In our previous work (e.g., Ref. [25]), the influence of E_{stop} on various observables was studied. It was found that the multiplicity of the final fragments does not depend on the chosen E_{stop}. As shown in Ref. [26], the average fragment multiplicity as a function of the excitation energy manifests the onset of multifragmentation, which occurs at excitation energies of approximately 3 MeV/nucleon. Thus, $E_{\mathrm{stop}} = 3$ MeV/nucleon was chosen in this work. In the GEMINI code, only the light-particle evaporation mode was considered. The excitation energy of the fragments can be calculated as

$$E^* = \frac{\sum_i U_i + \sum_i \frac{\left(\mathbf{p}_i - \mathbf{p}_{\mathrm{f}}\right)^2}{2m} - B\left(Z_{\mathrm{f}}, A_{\mathrm{f}}\right)}{A_{\mathrm{f}}}, \tag{4}$$

where U_i and $\mathbf{p}_i$ are the single-particle potential and momentum of the ith nucleon in the center of mass of the collision system, respectively. $\mathbf{p}_{\mathrm{f}}$ is the momentum of the corresponding fragment nucleon under the center of mass of the collision system. Z_{f}, and A_{f} are the charge number and mass number of the fragment, respectively. $B\left(Z_{\mathrm{f}}, A_{\mathrm{f}}\right)$ is the binding energy of a nucleus with a charge number Z_{f}

and mass number A_{f}. The summation is obtained for the nucleons belonging to the same fragment.

In our previous work, the validity of the theoretical approach was tested by comparing the calculated product yields and the experimental results of the ALADIN Collaboration. The calculations can reproduce the isotope distribution data and mean neutron-to-proton ratios of the light fragments [25].

3 Results and discussion

To study the isospin fractionation in the projectile fragmentations, it is helpful to compare the isospins between the gas phase (fragments of $Z<3$) and liquid phase (intermediate mass fragments and residues). For each reaction, more than 100,000 events were considered to ensure sufficient statistical accuracy. The measured free neutrons and protons came not only from the fragmenting stage, but also from the pre-equilibrium and secondary decay stages. The method proposed by Xu et al. was applied to estimate the ratio between the neutrons and protons emitted by the fragmenting source [8]. The yield ratio $M(Z, N)/M(N, Z)$ as a function of the binding energy difference $\triangle B$ for light mirror nuclei is given by

$$\frac{M(Z,N)}{M(N,Z)} \approx \frac{\rho_n}{\rho_p} e^{\triangle B/T} \frac{f_{Z,N}(T)}{f_{N,Z}(T)}, \tag{5}$$

where T is the temperature of the fragmenting system, and $f_{Z,N}(T)/f_{N,Z}(T)$ is the secondary decay factor. Figure 1 shows the analysis of the yield ratios of four pairs of mirror nuclei: ^{3}H/^{3}He, ^{7}Li/^{7}Be, ^{11}B/^{11}C, and ^{15}N/^{15}O, obtained from the projectile fragmentations in ^{124}Sn, ^{107}Sn + ^{120}Sn at 600 MeV/nucleon with b = 5 fm. For the IQMD calculations, there was no secondary decay; hence, no correction was required ($f_{Z,N}(T)/f_{N,Z}(T) = 1$). Fitting the yield ratios from the IQMD simulations with Eq. (5), we obtained ρ_n/ρ_p = 1.62 for ^{124}Sn, and 1.23 for ^{107}Sn. The larger ρ_n/ρ_p values than the projectile *N/Z* indicate the isospin fractionation. For calculations using IQMD+GEMINI, the yield ratios display a trend similar to Eq. (5). Only three pairs of mirror nuclei were analyzed because of the scarce production of ^{15}N and ^{15}O. Fitting the yield ratios obtained from IQMD+GEMINI using Eq. (5), the ρ_n/ρ_p = 1.32 for ^{124}Sn, and 1.03 for ^{107}Sn. In simulations with secondary decay, the extracted values of ρ_n/ρ_p were smaller than the projectile *N/Z* (1.48 for ^{124}Sn, and 1.14 for ^{107}Sn) and those without secondary decay. This indicates that the secondary decay distorts the ρ_n/ρ_p values. In other words, fitting the final fragments using Eq. (5), the extracted ρ_n/ρ_p does not reflect the isospin of the gas phase in the fragmentation. We also found that the momentum-dependent potential energy affects the yield ratio $M(Z, N)/M(N, Z)$, and the extraction of ρ_n/ρ_p.

Using ρ_n/ρ_p as the isospin observable, the symmetry energy dependence of the isospin fractionation in the projectile fragmentations of ^{124}Sn, ^{107}Sn + ^{120}Sn at 600 MeV/nucleon as well as ^{136}Xe, ^{124}Xe + ^{208}Pb at 1000 MeV/nucleon was studied. The results are shown in Figs. 2 and 3. It was found that the stiff symmetry energy results in a lower ρ_n/ρ_p value than the soft one. Because of the smaller isospin asymmetries, this symmetry energy dependence is relatively weak for ^{107}Sn and ^{124}Xe. The projectile-like source was heated but not compressed during the pre-equilibrium stage. It is supposed that the nuclear gas (light particles) was steamed out from the periphery of the source, where the density is lower than the normal density. The smaller symmetry energy ($\gamma_i = 2$) at subnormal

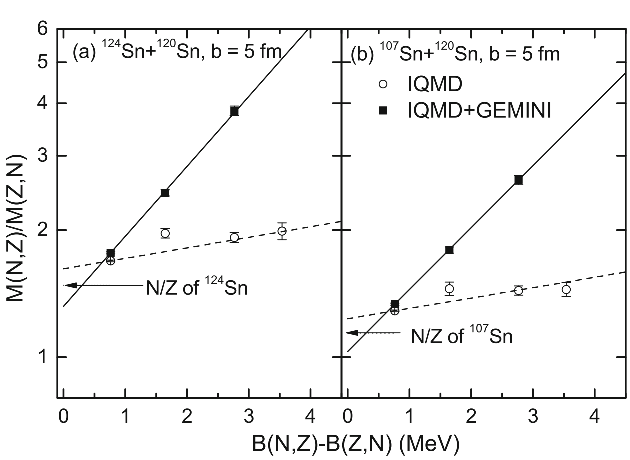

Fig. 1 The yield ratios of the mirror nuclei produced in the projectile fragmentations of ^{124}Sn, ^{107}Sn + ^{120}Sn at 600 MeV/nucleon with $b = 5$ fm

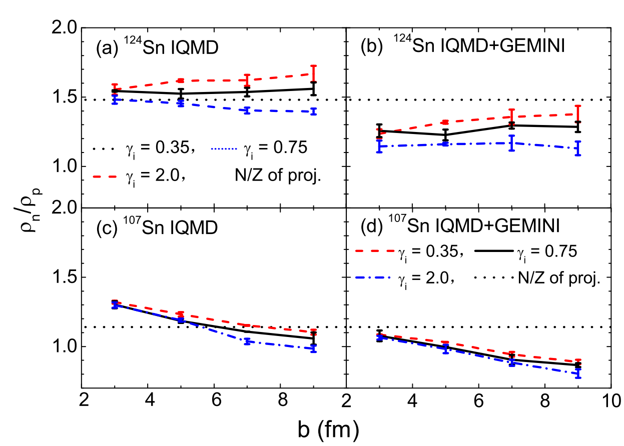

Fig. 2 (Color online) Impact parameter dependence of ρ_n/ρ_p values extracted from the yield ratios of the mirror nuclei produced in the projectile fragmentations of ^{124}Sn, ^{107}Sn + ^{120}Sn at 600 MeV/nucleon. See text for the extracted method

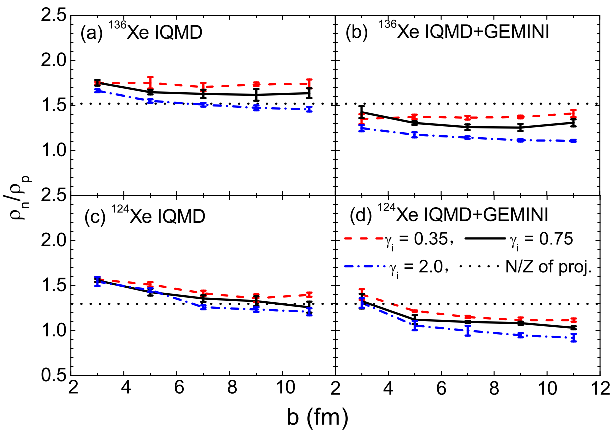

Fig. 3 (Color online) Same as Fig. 2 but for ^{136}Xe, ^{124}Xe + ^{208}Pb at 1000 MeV/nucleon

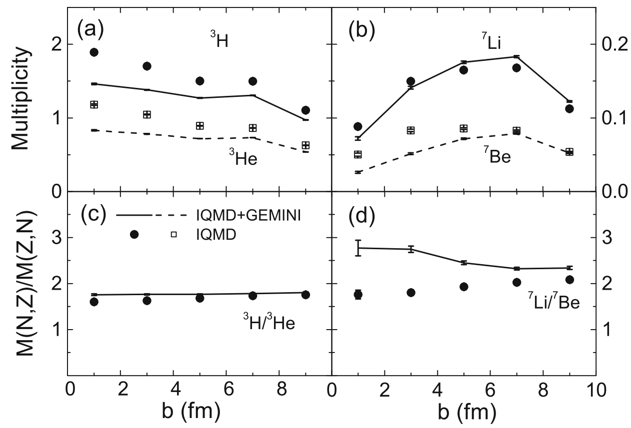

Fig. 4 The yields and ratios of two pairs of mirror nuclei, ^{3}H/^{3}He, ^{7}Li/^{7}Be produced in the projectile fragmentation of ^{124}Sn + ^{120}Sn at 600 MeV/nucleon and γ_i = 0.35

density provides a smaller repulsive force for neutrons and an attractive force for protons in the neutron-rich system. This leads to a smaller ρ_n/ρ_p in the gas phase (Figs. 2 and 3), leaving a neutron-rich liquid phase.

Figures 2 and 3 depict the impact parameter dependence of the isospin fractionation. The impact parameter dependence of the ρ_n/ρ_p values is weak within the uncertainties for ^{124}Sn and ^{136}Xe. However, for ^{107}Sn and ^{124}Xe, the general trend is a decreasing ρ_n/ρ_p with increasing impact parameter. The ^{107}Sn is the neutron-deficient nucleus. It is known that ^{124}Xe is the stable nucleus, whose neutron number is the lowest in stable Xe nuclei. The isospin fractionation of the neutron-deficient system leads to a smaller value of ρ_n/ρ_p in the gas phase than that of the initial *N*/*Z* value. The anomalous ρ_n/ρ_p values may be related to the isospin diffusion between the projectile and target.

The ratio between mirror nuclei yields is an isospin observable. Figure 4 shows the yields and ratios of two pairs of mirror nuclei, ^{3}H/^{3}He, ^{7}Li/^{7}Be, produced in the projectile fragmentations of ^{124}Sn + ^{120}Sn at 600 MeV/nucleon. The calculations with and without the GEMINI code were compared. The yields of the prefragments (by IQMD) contain information on the isospin fractionation. However, some information will be lost during the secondary decay stage where the binding energies rule. The binding energies depend on the symmetry energy at the normal density rather than at a subnormal density. In the decay process, two factors affect the yields of ^{3}H and ^{3}He. First, the heavier nuclear decay becomes ^{3}H and ^{3}He. Second, excited ^{3}H and ^{3}He decay into lighter nuclei, reducing ^{3}H and ^{3}He. The calculation results suggest that the latter plays a dominant role. This is the reason why the calculated value of IQMD+GEMINI is lower than that of IQMD, as shown in Fig. 4. We discussed this phenomenon in Fig. 8(d) of Ref. [25]. In the figure, it is shown that the yields of the ^{3}H, ^{3}He, and ^{7}Be nuclei are reduced by secondary decay. Owing to the stronger bond for the ^{7}Li nucleus, its yields do not change significantly after the secondary decay. As a result, the secondary decay effects of the yield ratio are weak for ^{3}H/^{3}He, but strong for ^{7}Li/^{7}Be (as shown in Fig. 4c, d). In addition, as mentioned in Ref.[15], the momentum-dependent potential energy also affects the yield of light particles (^{3}H, ^{3}He, ^{7}Li, ^{7}Be) as well as the yield ratio.

The yield ratios of the mirror nuclei ^{3}H/^{3}He were used to study the dependence of the projectile fragmentation on symmetry energy. Two soft (γ_i = 0.35 and 0.75) and stiff (γ_i = 2) symmetry energies were applied in the IQMD+GEMINI model to perform the collisions of ^{124}Sn, ^{107}Sn + ^{120}Sn at 600 MeV/nucleon. In Fig. 5, the yield ratio calculations of ^{3}H/^{3}He are shown as a function of the normalized bound charge Z_{bound}/Z_p as well as the impact

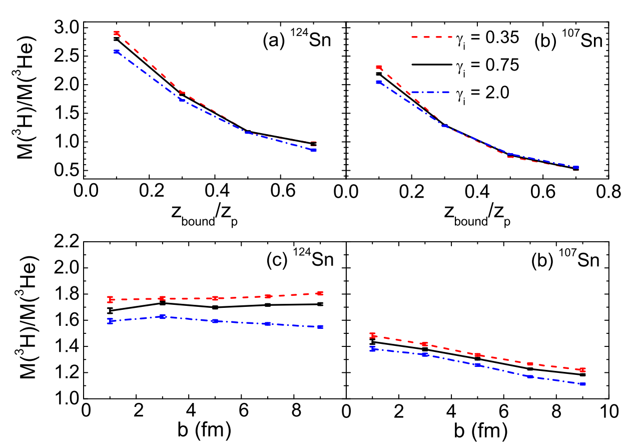

Fig. 5 (Color online) Yield ratios of mirror nuclei ^{3}H/^{3}He produced in the projectile fragmentations of ^{124}Sn, ^{107}Sn + ^{120}Sn at 600 MeV/nucleon

parameter b. The Z_{bound} is defined as the sum of the fragment charges of all fragments with Z_i [34]. The bound charge monotonically increased with increasing impact parameter and was applied for event sorting in the experiment. The symmetry energy dependence and impact parameter dependence of ρ_n/ρ_p (Figs. 2 and 3) were also determined for the yield ratios of ^{3}H/^{3}He. First, the stiff symmetry energy resulted in smaller yield ratios of ^{3}H/^{3}He compared with the soft cases. The symmetry energy dependence is weak for ^{107}Sn, but relatively strong for ^{124}Sn. Second, owing to the coexistence of isospin diffusion and isospin fractionation, the yield ratios of ^{3}H/^{3}He for ^{107}Sn decreased with increasing b, but those for ^{124}Sn are similar for all b. Compared with the isospin observable ρ_n/ρ_p, the yield ratios of ^{3}H/^{3}He have two advantages, i.e., smaller uncertainty and weak secondary decay effect. The yield ratios of ^{3}H/^{3}He for both ^{107}Sn and ^{124}Sn decreased with increasing normalized bound charge Z_{bound}/Z_p. However, the difference between these two fragmenting systems is more evident in peripheral collisions. We can still see the effect of different symmetry energies within the range of error bar coverage.

The secondary decay effects can be further minimized by using the double ratio of ^{3}H/^{3}He ratios between two systems with different isospin asymmetry of projectiles. The double yield ratio (DR) is defined as

$$\mathrm{DR} = \frac{\left.\frac{M(^3\mathrm{H})}{M(^3\mathrm{He})}\right|_{124}}{\left.\frac{M(^3\mathrm{H})}{M(^3\mathrm{He})}\right|_{107}}, \tag{6}$$

where the subscripts 124 and 107 refer to the ^{124}Sn + ^{120}Sn and ^{107}Sn + ^{120}Sn collisions, respectively. For ^{136}Xe, ^{124}Xe + ^{208}Pb collisions at 1000 MeV/nucleon, a similar DR was defined, but with subscripts of 136 and 124. Figures 6 and 7 show the calculated DR for projectile fragmentations in ^{124}Sn, ^{107}Sn + ^{120}Sn collisions at 600 MeV/nucleon, and ^{136}Xe, ^{124}Xe + ^{208}Pb collisions at 1000 MeV/nucleon. The DR values increased with increasing b and Z_{bound}/Z_p. A comparison of the DR values obtained from the calculations with different symmetry energies indicates that DR can be used as an isospin observable. The isospin observable DR allows one to constrain the symmetry energy by the peripheral collision at hundreds of MeV/nucleon. Using the bound charge in event sorting, the symmetry energy dependence is stronger in the region of a large bound charge. The symmetry energy also affects the error bar coverage.

To further test our theory, ^{136}Xe, ^{124}Xe + ^{208}Pb collisions are shown in Fig. 7. As mentioned above, isospin diffusion leads to a weak target dependence of the fragmenting source during peripheral collision. Thus, it is expected that the DR value will increase (i.e., a larger difference between the neutron-rich and neutron-deficient systems) with increasing impact parameter. Because the number of events is proportional to b^2, the peripheral events are greater than the central events. The stiff symmetry energy results in a smaller ρ_n/ρ_p value in the gas phase compared with the soft case.

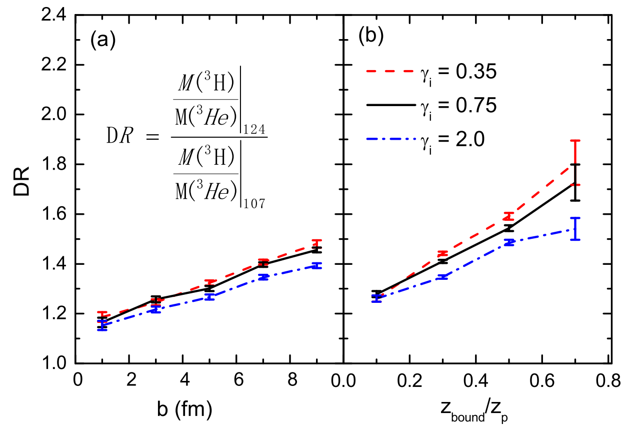

Fig. 6 (Color online) Double yield ratios (DR) of mirror nuclei ^{3}H/^{3}He produced in the projectile fragmentations of ^{124}Sn, ^{107}Sn + ^{120}Sn at 600 MeV/nucleon

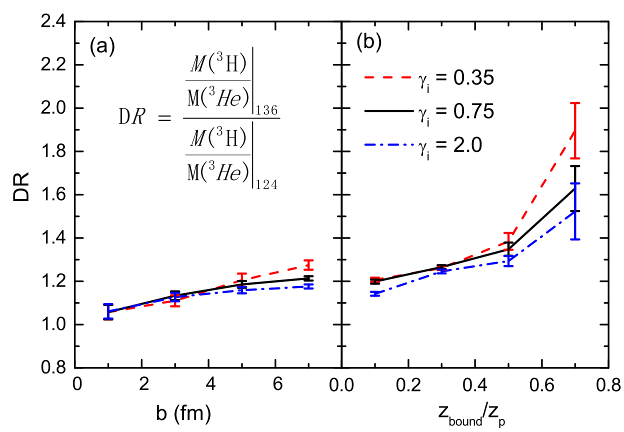

Fig. 7 (Color online) Double yield ratios (DR) of mirror nuclei ^{3}H/^{3}He produced in the projectile fragmentations of ^{136}Xe, ^{124}Xe + ^{208}Pb at 1000 MeV/nucleon

4 Conclusion

The isospin fractionations in ^{124}Sn, ^{107}Sn + ^{120}Sn at 600 MeV/nucleon, and ^{136}Xe, ^{124}Xe + ^{208}Pb at 1000 MeV/nucleon were investigated by the IQMD model coupled with the statistical code GEMINI. The yield ratio as a function of the binding energy difference for light mirror nuclei ^{3}H/^{3}He, ^{7}Li/^{7}Be, ^{11}B/^{11}C, and ^{15}N/^{15}O was applied to estimate the ratio between neutrons and protons in the gas of the fragmenting system. By comparing the estimated values obtained from the calculations with and without the GEMINI code, it was found that the secondary decay distorts the signal of the isospin fractionation. Using the neutron/proton ratio in the gas as the isospin observable, the symmetry energy dependence of the isospin fractionation was studied. The symmetry energy dependence was weak for ^{107}Sn and ^{124}Xe fragmentations, but evident for ^{124}Sn and ^{136}Xe fragmentations.

Because of the secondary decay effects, the neutron/proton ratio in the gas is not a robust isospin observable. Instead, the yield ratio of the light mirror nuclei ^{3}H/^{3}He as well as its double ratio between two systems with different isospin asymmetries of the projectiles was considered. As a result of the small binding energy difference, the yield ratio of ^{3}H/^{3}He was slightly distorted by the secondary decay. Distortions caused by secondary decay can be minimized by using the double ratio between two systems with different isospin asymmetries of the projectiles. The DR can be used as an isospin observable. Stiff symmetry energy generally leads to a smaller value of the gas, in contrast to the soft case. It is beneficial to obtain high-precision data because the counting for peripheral collisions is larger than for central collisions.

References

1. K. Carlson, Lipoprotein fractionation. J. Clin. Pathol. **s1–5**, 32–37 (1973). https://doi.org/10.1136/jcp.s1-5.1.32
2. R. Park, S. Epstein, Carbon isotope fractionation during photosynthesis. Geochim. Cosmochim. Acta **21**, 110–126 (1960). https://doi.org/10.1016/s0016-7037(60)80006-3
3. C. Ducoin, P. Chomaz, F. Gulminelli, Isospin fractionation: equilibrium versus spinodal decomposition. Nucl. Phys. A **781**, 407–423 (2007). https://doi.org/10.1016/j.nuclphysa.2006.11.047
4. Z.H. Li, W. Zuo, G.C. Lu, Phase transition of hot nuclear matter. Chin. Phys. Lett. **21**, 29–32 (2004). https://doi.org/10.1088/0256-307x/21/1/009
5. T.Z. Yan, S. Li, Impact parameter dependence of the yield ratios of light particles as a probe of neutron skin. Nucl. Sci. Tech. **30**, 43 (2019). https://doi.org/10.1007/s41365-019-0572-8
6. X.M. Zhang, W.L. Qian, R.K. Su, Liquid–gas phase transition for asymmetric nuclear matter in the Zimanyi–Moszkowski model. Chin. Phys. Lett. **21**, 1240–1242 (2004). https://doi.org/10.1088/0256-307x/21/7/015
7. J. Randrup, S.E. Koonin, The disassembly of nuclear matter. Nucl. Phys. A **356**, 223–234 (1981). https://doi.org/10.1016/0375-9474(81)90124-x
8. H.S. Xu, M.B. Tsang, T.X. Liu et al., Isospin fractionation in nuclear multifragmentation. Phys. Rev. Lett. **85**, 716–719 (2000). https://doi.org/10.1103/physrevlett.85.716
9. B.A. Li, Neutron–proton differential flow as a probe of isospin-dependence of the nuclear equation of state. Phys. Rev. Lett. **85**, 4221–4224 (2000). https://doi.org/10.1103/physrevlett.85.4221
10. A. Ono, P. Danielewicz, W.A. Friedman et al., Isospin fractionation and isoscaling in dynamical simulations of nuclear collisions. Phys. Rev. C **68**, 051601 (2003). https://doi.org/10.1103/physrevc.68.051601
11. M. Zhang, Z.G. Xiao, B.A. Li et al., Systematic study of the π-/π+ ratio in heavy-ion collisions with the same neutron/proton ratio but different masses. Phys. Rev. C **80**, 034616 (2009). https://doi.org/10.1103/physrevc.80.034616
12. B.A. Li, L.W. Chen, H.R. Ma et al., Differential isospin-fractionation in dilute asymmetric nuclear matter. Phys. Rev. C **76**, 051601 (2007). https://doi.org/10.1103/physrevc.76.051601
13. J. Xu, L.W. Chen, B.A. Li, Thermal properties of asymmetric nuclear matter with an improved isospin- and momentum-dependent interaction. Phys. Rev. C **91**, 014611 (2015). https://doi.org/10.1103/physrevc.91.014611
14. J.Y. Liu, W.J. Guo, Y.Z. Xing et al., Isospin effect of Coulomb interaction on the dissipation and fragmentation in intermediate energy heavy ion collisions. Phys. Rev. C **70**, 034610 (2004). https://doi.org/10.1103/physrevc.70.034610
15. J.Y. Liu, W.J. Guo, Y.Z. Xing et al., Isospin momentum-dependent interaction and its role on the isospin fractionation ratio in intermediate energy heavy ion collisions. Chin. Phys. Lett. **22**, 65–68 (2004). https://doi.org/10.1088/0256-307x/22/1/019
16. W.J. Guo, J.Y. Liu, Y.Z. Xing, Effect of Coulomb interaction on the isospin fractionation process. Chin. Phys. Lett. **21**, 1495–1497 (2004). https://doi.org/10.1088/0256-307x/21/8/022
17. Ad R. Raduta, F. Gulminelli, Isospin dependent thermodynamics of fragmentation. Phys. Rev. C **75**, 044605 (2007). https://doi.org/10.1103/physrevc.75.044605
18. D.Q. Fang, W.Q. Shen, J. Feng et al., Isospin effect of fragmentation reaction on the isotopic distribution produced in intermediate energy heavy ion collisions. Chin. Phys. Lett. **17**, 267–269 (2000). https://doi.org/10.1088/0256-307x/17/4/012
19. C.W. Ma, C.Y. Qiao, T.T. Ding et al., Temperature of intermediate mass fragments in simulated 40Ca+40Ca reactions around the Fermi energies by AMD model. Nucl. Sci. Tech. **27**, 111 (2016). https://doi.org/10.1007/s41365-016-0112-8
20. Z.Q. Feng, Nuclear dynamics and particle production near threshold energies in heavy-ion collisions. Nucl. Sci. Tech. **29**, 40 (2018). https://doi.org/10.1007/s41365-018-0379-z
21. Y.J. Wang, C.C. Guo, Q.F. Li et al., ^{3}H/^{3}He ratio as a probe of the nuclear symmetry energy at sub-saturation densities. Eur. Phys. J. A **51**, 37 (2015). https://doi.org/10.1140/epja/i2015-15037-8
22. C.W. Ma, Y.L. Zhang, S.S. Wang et al., A model comparison study of fragment production in 140 A MeV ^{58,64}Ni + ^{9}Be reactions. Chin. Phys. Lett. **32**, 072501 (2015). https://doi.org/10.1088/0256-307x/32/7/072501
23. P. Zhou, W.D. Tian,Y.G. Ma et al., The influence of multi-step sequential decay on isoscaling and fragment isospin distribution in GEMINI simulation. Chin. Phys. Lett. **28**, 062101 (2011). https://doi.org/10.1088/0256-307x/28/6/062101
24. Z.F. Zhang, D.Q. Fang, Y.G. Ma, Decay modes of highly excited nuclei. Nucl. Sci. Tech. **29**, 78 (2018). https://doi.org/10.1007/s41365-018-0427-8
25. J. Su, W. Trautmann, L. Zhu, et al., Dynamical properties and secondary decay effects of projectile fragmentations in Sn124, Sn107+Sn120 collisions at 600 MeV/nucleon. Phys. Rev. C **98**, 014610 (2018). https://doi.org/10.1103/physrevc.98.014610
26. B. Borderie, M.F. Rivet, Nuclear multifragmentation and phase transition for hot nuclei. Prog. Part. Nucl. Phys. **61**, 551–601 (2008). https://doi.org/10.1016/j.ppnp.2008.01.003
27. J. Su, L. Zhu, C.C. Guo et al., Isospin dependence of the projectile fragmentation at hundreds MeV/nucleon. Chin. Phys. Lett. **44**, 094105 (2020). https://doi.org/10.1088/1674-1137/44/9/094105
28. J. Su, L. Zhu, C.Y. Huang et al., Correlation between symmetry energy and effective k-mass splitting with an improved isospin-

and momentum-dependent interaction. Phys. Rev. C **94**(3), 034619 (2016). 10.1103/PhysRevC.94.034619
29. J. Su, L. Zhu, C.Y. Huang et al., Effects of symmetry energy and effective k-mass splitting on central ^{96}Ru (^{96}Zr) + ^{96}Zr (^{96}Ru) collisions at 50 to 400 MeV/nucleon. Phys. Rev. C **96**(2), 024601 (2017). 10.1103/PhysRevC.96.024601
30. J. Cugnon, D. L'Hôte, J. Vandermeulen, Simple parametrization of cross-sections for nuclear transport studies up to the GeV range. Nucl. Instrum. Methods Phys. Res. Sect. B **111**, 215–220 (1996). https://doi.org/10.1016/0168-583x(95)01384-9
31. D.D.S. Coupland, W.G. Lynch, M.B. Tsang et al., Influence of transport variables on isospin transport ratios. Phys. Rev. C **84**, 054603 (2011). https://doi.org/10.1103/physrevc.84.054603
32. M. Papa, Many-body correlations in semiclassical molecular dynamics and Skyrme interaction. Phys. Rev. C **87**, 014001 (2013). https://doi.org/10.1103/PhysRevC.87.014001
33. M. Papa, G. Giuliani, A. Bonasera, Constrained molecular dynamics II: an N-body approach to nuclear systems. J. Comput. Phys. **208**, 403–415 (2005). https://doi.org/10.1016/j.jcp.2005.02.032
34. R. Ogul, A.S. Botvina, U. Atav, Isospin-dependent multifragmentation of relativistic projectiles. Phys. Rev. C **83**, 024608 (2011). 10.1103/PhysRevC.83.024608